Earth and Planetary Science Letters 467 (2017) 57–63

Contents lists available at ScienceDirect

Earth and Planetary Science Letters

www.elsevier.com/locate/epsl

The identification and significance of pure sediment-derived granites

Thomas N. Hopkinson [a,*], Nigel B.W. Harris [a], Clare J. Warren [a], Christopher J. Spencer [c], Nick M.W. Roberts [b], Matthew S.A. Horstwood [b], Randall R. Parrish [b], EIMF [d]

[a] School of Environment, Earth and Ecosystem Sciences, Open University, Milton Keynes, MK7 6AA, UK
[b] NERC Isotope Geosciences Laboratory, British Geological Survey, Keyworth, NG12 5GG, UK
[c] Earth Dynamics Research Group, TIGeR (The Institute of Geoscience Research), Department of Applied Geology, Curtin University, Perth, Australia
[d] Edinburgh Ion Microprobe Facility, University of Edinburgh, Edinburgh, EH9 3FE, UK

ARTICLE INFO

Article history:
Received 24 August 2016
Received in revised form 19 January 2017
Accepted 13 March 2017
Available online xxxx
Editor: D. Vance

Keywords:
granite
S-type
Himalaya
oxygen
hafnium
geochronology

ABSTRACT

The characterization of the geochemical reservoirs of the Earth's continental crust, including the determination of representative upper and lower crustal compositions, underpins our understanding of crustal evolution. The classic I- and S-type granite classification has often been invoked to distinguish between melts derived from igneous protoliths and those derived from the melting of a sedimentary source. Recent geochemical studies suggest that most granites, even those cited as typical examples of 'S-type', show evidence for a mixture of mantle and upper crustal sources, thereby implying that granite formation is evidence for overall crustal growth. We have examined the source of leucogranite bodies in one of the world's youngest collisional orogens using novel zircon techniques that can resolve the presence of even minor mantle contributions. 232 zircons from 12 granites from the Bhutan Himalaya were analysed by *in-situ* techniques for O, Hf and U–Pb isotopic signatures. In combination with data from the granite host rocks, our data show that the Himalayan leucogranites were derived solely from metamorphosed crustal sediments, and do not record any mantle contribution. This finding is consistent with the time-lag between crustal thickening and widespread crustal melting, and the heat-producing capacities of the pelitic source rocks. We conclude that Himalayan leucogranites provide a more suitable type locality for 'S-type' granites than the Lachlan area in South-East Australia where the term was first defined. The Himalayan leucogranites therefore provide evidence that syn-orogenic melting during collisional events does not necessarily result in crustal growth. Importantly, crustal growth models should not always assume that crustal growth is achieved during collisional orogenesis.

1. Introduction

Crustal melting and the formation of granitic magmas are key processes in crustal evolution, facilitating transfer of heat and volatile elements within the crust and contributing to mechanical weakening of the crust throughout episodes of mountain building. Granites are particularly associated with crustal melting at convergent plate margins where crustal rocks are thickened, heated and deformed. Whilst individual granite bodies may have multiple melt sources, it has become well-established that most granites can be classified as either 'I-type' (those with mainly igneous, including mantle, sources), or 'S-type' (those with mainly sedimentary sources) as first described formally in the Lachlan Fold Belt of south-east Australia (Chappell and White, 1974; McCulloch and Chappell, 1982). This simple classification, later extended to include further categories such as A-type (Loiselle and Wones, 1979), has arguably become the most widely used scheme for granite classification.

Since the initial study, further bulk-rock isotope results showed that the S-types granites from the Lachlan fold belt have significant mantle input and thus are not 'pure' crustal melts (Gray, 1984; Collins, 1996; Healy et al., 2004). Nevertheless, Lachlan granites classified as 'S-type' continue to be taken as a paragon of sediment-sourced magmas (Teng et al., 2004; Bea et al., 2007; Savage et al., 2012). A misunderstanding of the nature of 'S-type' granites may lead to misleading conclusions in interpreting the role of granite petrogenesis or geochemical behaviour during crustal melting. For example, based on the assumption that the Lachlan 'S-type' granites represent the crustal end-member of granitic rocks, minor differences in the bulk-rock Si isotope composition of 'I-type' and 'S-type' granites led researchers to conclude that Si isotopes are not sensitive to sedimentary input (Savage et al., 2012). A further study documenting the similarity between

* Corresponding author.
E-mail address: t.n.hopkinson@gmail.com (T.N. Hopkinson).

http://dx.doi.org/10.1016/j.epsl.2017.03.018

bulk-rock Li isotopic compositions of Lachlan S-type granites and their associated sedimentary rocks suggested that Li-isotope fractionation during crustal melting was negligible (Teng et al., 2004). Neither conclusion is necessarily valid if the S-type samples analysed are in fact mixtures of both mantle and crustal melt sources.

Despite suggestions from field evidence, there is yet there is no conclusive chemical evidence that coherent granite bodies, as opposed to the leucosome component in migmatites (Inger and Harris, 1993), may be derived entirely from melting sediments. The recognition of such bodies will provide representative compositions of pure crustal melts for future geochemical studies. The establishment of the total volume of pure crustal melts of different ages are critical for calculating the global magmatic budget, as these magmas have not contributed to net crustal growth.

The chemical recognition of pure crustal melts also carries implications for the thermal and tectonic evolution of orogenic belts. Two processes can control magma generation during orogenesis. During collision, hot mantle material may firstly become directly entrained in the lower crust, which will ultimately cause advective heating and crustal melting. These melts will incorporate a mantle chemical signature. This process is more likely during slow collisions with some element of lateral extension. In contrast, rapid collisions result in melting when a thick pile of radiogenic pelitic to semi-pelitic sedimentary rocks is tectonically buried deep enough to allow them to melt extensively without an external heat source. The distribution and timing of melting depends on the heat production of the sediments (abundances of radioactive elements U, Th and K), the distribution and thickness of fertile lithologies, and to some extent, the geometry of the collision (Patiño-Douce et al., 1990).

The origin of the High Himalayan leucogranites is therefore intrinsically associated with the geodynamic and thermal evolution of the India–Asia collision. Although collision and crustal thickening is widely held to have occurred at 50–55 Ma (Najman et al., 2010) and may have begun as early as 59 ± 1 Ma (Hu et al., 2015), an alternative view for major collision at ~34 Ma has also been proposed (Aitchison et al., 2007). Given that the High Himalayan leucogranite bodies formed at ~20 Ma, the competing models allow timespans varying from >30 million yrs (for early Eocene collision) and ~14 million yrs (for collision on the Eocene–Oligocene boundary). For widespread melting to occur in the mid crust, temperatures must reach values of at least ~700 °C (the temperature of the muscovite dehydration reaction; Harris et al., 1995). Thermal models for orogenic evolution require a time period of at least 20 to 30 million yrs between collision and melting for all realistic values of heat production and sedimentary thicknesses and assuming no advective heat source (Medvedev and Beaumont, 2006). Acceleration of heating could only occur if additional heat sources were available, such as from rising melts from the lower crust or mantle, or from shear heating along discrete thrusts. In the Himalaya, there is little to no field or chemical evidence for such extra heat sources (Harris and Massey, 1994). Hence in the Himalaya, the 'young' collision model requires a widespread mantle melt component to provide advective heating to accelerate the rate of Miocene magmatism. The absence of any recognized intermediate or mafic intrusions across the High Himalaya therefore suggests an early collision, unless a mantle component can be identified in the leucogranite melts themselves.

Traditionally, granite geochemical studies have been based on bulk-rock data that provide averaged information of all component mineral phases and therefore fail to resolve contributions from discrete individual sources. Furthermore, bulk-rock samples may not reflect the original composition of the crystallised melt for a variety of reasons, ranging from incomplete separation of magma from restitic or peritectic phases (due to the high viscosity of granite magmas and to the small density contrast between such melts and silicate phases), or to the modification of the crystallised granite by post-magmatic processes such as hydrothermal activity and weathering.

Advances in *in-situ* micro-analysis techniques for the determination of e.g. U–Pb, Lu–Hf and O isotopic compositions in accessory minerals have revolutionized approaches to assessing the evolution of the continental crust, and granite petrogenesis (Kemp et al., 2006, 2007; Appleby et al., 2010; Roberts and Spencer, 2014). Zircon is a common accessory mineral in granitic rocks and retains geochemical information about the evolution of its host melt. For typical peraluminous melt, <100 ppm zirconium is needed to saturate the melt and crystallise zircon (Hanchar and Watson, 2003). Therefore Zr saturation is likely reached early in the magmatic evolution of such granites, the time at which it is most likely to retain the record of its source.

The three isotope systems combine to inform both timing and melt source. U–Pb is a well-documented geochronometer that records the timing of zircon crystallisation, while the Lu–Hf and O systems together combine to record the geochemical characteristics of the source. Lu–Hf is a radiogenic isotope system that records the average age of mantle extraction of the melt source. In general, samples with more negative εHf values were extracted from the mantle further back in time (a deviation in $^{176}Hf/^{177}Hf$ from the chondritic uniform reservoir (CHUR) value in parts per ten thousand). The behaviour of oxygen isotopes in rocks and minerals provides a stable-isotope proxy for the extent of sedimentary recycling in the sample source. Oxygen isotopes are fractionated during low-temperature processes such as subaerial weathering. Magmas that incorporate this supracrustal material will inherit a heavier $\delta^{18}O$ signature (or greater $^{18}O/^{16}O$ value) with respect to the Vienna Standard Mean Ocean Water (VSMOW; in parts per thousand).

Hf–O measurements of zircon from granitic rocks from the Lachlan type area have suggested that 'S-type' granitic and volcanic rocks cannot be derived from a single protolith and instead incorporate between 20 and 75% of material from a mantle source (Kemp et al., 2006, 2007). A more recent Hf–O isotopic study of zircons in 'S-type' granites from the Caledonian orogeny report a range of zircon compositions including those with typical 'mantle-like' O isotope signatures (Appleby et al., 2010). Thus on the basis of published zircon Hf–O studies it appears that many granites, including those traditionally classified as 'S-type', are derived from mixed evolved and juvenile sources, generally interpreted as crustal and mantle-sources respectively.

We have analysed the chemical composition of zircons from 12 peraluminous Oligocene to Miocene (33–11 Ma) leucogranites exposed in the eastern Himalayan orogen in Bhutan (Fig. 1). The granites represent a range of mineralogical types, with seven two-mica (1G03, 3A03, 4D01, 1247, 1251, CWB16 and CWB23), three tourmaline (1G02, 3A04, 1215) and two garnet leucogranites (1D01, 3A02) studied. These leucogranites intrude amphibolite-facies metasediments of primarily Neoproterozoic source age, the Greater Himalayan Sequence (GHS) (Ahmad et al., 2000; Gehrels et al., 2011). Structurally below the GHS is the Lesser Himalayan Sequence (LHS), a primarily Paleoproterozoic-sourced stack of metasediments (Ahmad et al., 2000; Gehrels et al., 2011). Both sequences comprise a mix of orthogneiss, carbonate and quartzite compositions with a minor pelite component. The pelitic assemblages are significantly more fusible and therefore provide appropriate source materials for anatectic melts where temperatures are relatively low (<750 °C, Patiño Douce and Johnston, 1991). Bulk-rock isotope geochemical data from similar High Himalayan leucogranites exposed elsewhere in the Himalaya suggest that they formed by partial melting of the GHS pelitic lithologies into which they now intrude (Le Fort et al., 1987; Harris et al., 1995). The granites are therefore appropriate for testing the hypothesis that

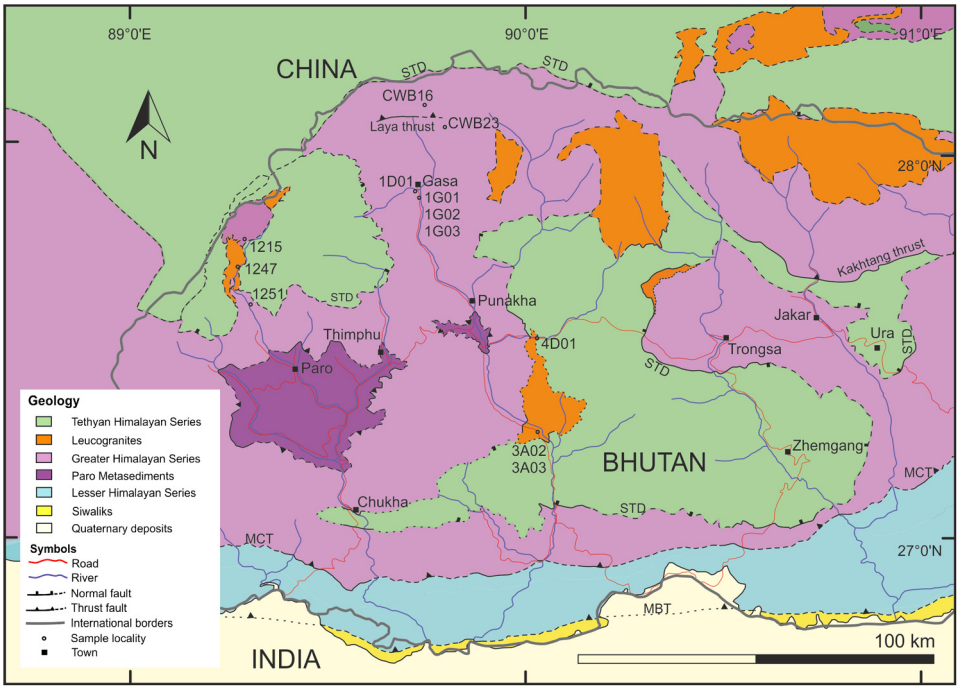

Fig. 1. Geological map of western and central Bhutan, adapted from Greenwood et al. (2016) showing sample localities. STD = South Tibetan Detachment, MCT = Main Central Thrust, MBT = Main Boundary Thrust, MFT = Main Frontal Thrust.

they represent pure crustal melts, and that these melts provide geochemical signatures that characterise their sedimentary source.

2. Methods

Zircons were separated, mounted in epoxy disks, polished down to equatorial sections and imaged by cathodoluminescence using standard techniques. Oxygen isotope analyses were performed on a Cameca 1270 ion microprobe at the Edinburgh ion microprobe facility (EIMF). A ~5 nA primary $^{133}Cs^{+}$ beam was used with a 10 µm spot size. Secondary ions were extracted at 10 kV. ^{16}O and ^{18}O ions were counted simultaneously on duel Faraday cups. 40 s of pre-sputtering was employed prior to each analysis, followed by automatic secondary beam and entrance slit centring, and finally data collection in two blocks of ten cycles, with a total count time of 80 s. Internal precision of each analysis is <0.2 per mil. Zircon '91500' (Wiedenbeck et al., 2004) and a laboratory internal zircon standard were used to correct for drift, instrument mass fractionation and daily standard reproducibility.

Following O isotope analysis, U–Pb and Hf isotopic analysis were performed at the NERC Isotope Geosciences Laboratory using a Nu Instruments Nu Plasma MC–ICP–MS coupled to a New Wave Research (NWR) 193ss Nd:YAG laser and a Thermo Neptune Plus MC–ICP–MS coupled to a NWR 193UC excimer laser, respectively. Hf ablation pits overlapped U–Pb pits, which in turn overlie the O-isotope pits. For U–Pb analyses, spot sizes were 25 µm, performed at 5 Hz and 2 J/cm^2 fluence, with a 30 s ablation time. For Hf isotope analyses, spot sizes were 35 µm, performed at 10 Hz and 6–7 J/cm^2. Normalisation was achieved with standard sample bracketing to zircon '91500' (Wiedenbeck et al., 1995) for U–Pb, and zircon 'Mud Tank' (Woodhead and Hergt, 2005) for Hf isotopes. Validation used zircons GJ-1 (Jackson et al., 2004) for U–Pb data and Plešovice (Sláma et al., 2008) for Hf isotope data. Data were carefully screened after each analysis for inadvertent analytical mixing between different growth zones.

Hf isotope ratios for Himalayan-age zircon rims were age-corrected to 20 Ma, an average age for Himalayan leucogranite samples, rather than their precise ages as recorded by the U–Pb data (between 33–11 Ma). Any age-scatter caused by Pb-loss is difficult to detect at such a young age, and therefore to avoid problems in Hf age correction caused by incorrect ages, we considered it more prudent to correct all the data to a single age. The difference between εHf_t and εHf_{20} for any given analysis lies within the quoted uncertainty.

Further details are given in the supplementary information. More details of the O, U–Pb, and Hf methods employed are detailed in Spencer et al. (2015).

3. Results

In-situ secondary ion mass spectrometry (SIMS) and laser ablation MC–ICP–MS analyses comprising 260 O, Hf and U–Pb isotopic analyses were conducted on 232 individual zircons recovered from 12 samples of Himalayan leucogranite. Of these, 80 spots yielded pre-Himalayan or mixed ages (1900–400 Ma), identifying inherited cores where $\delta^{18}O$ and εHf compositions predate partial melting during the Himalayan orogeny. The remaining 180 spots yielded Himalayan ages between 33–11 Ma; full data are supplied in supplementary Tables 1 and 2.

Age-corrected (to 20 Ma) εHf_{20} of all Himalayan-aged samples varies between −8.7 and −29.8, and $\delta^{18}O$ between 6.9‰ and 12.5‰ (Fig. 2). Of these analyses, 97% lie within uncertainty of the GHS O–Hf compositional range (calculated from whole rock $\delta^{18}O$ and Nd isotope data, see figure caption; Massey et al., 1994a, 1994b; Harris and Massey, 1994; Vervoort and Blichert-Toft, 1999; Lackey et al., 2005). In addition, all young zircon rims record more negative εHf_{20} values than the maximum values recorded by GHS zircons. Zircon data from some samples cluster densely (e.g. 1D01, 3A03). Samples 1G02 and CWB16 show variations in zircon εHf_{20} that are greater than analytical uncertainty, but $\delta^{18}O$ values conversely show little variation. In contrast, zircons in other samples, including 4D01, 1215 and 1247, show variation in $\delta^{18}O$ while εHf_{20} values remain relatively constant. Only one sample, 1G03, contained zircons that yielded significant variation in both isotope systems, with εHf_{20} varying between −30 and −15 and $\delta^{18}O$ between 7.1‰ and 8.1‰.

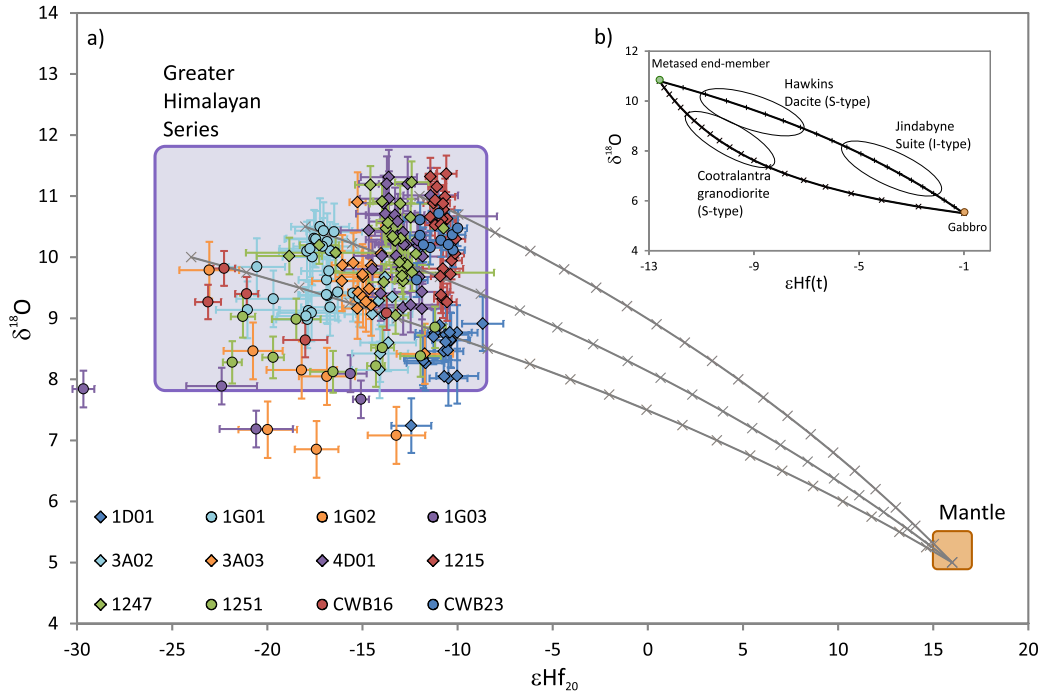

Fig. 2. a) $\delta^{18}O$–εHf_{20} isotope arrays for Oligocene to Miocene-aged zircons and zircon rims compared to possible mixing lines generated by binary mixing between potential GHS sources and the mantle (ticks show mixing at 5% intervals). The range of isotopic values from bulk rock GHS analyses (the likely source of melting) and the depleted mantle have also been plotted for reference. The GHS whole-rock εHf range is calculated from whole rock εNd (Harris and Massey, 1994) using the correlation of Vervoort and Blichert-Toft (1999). Whole-rock GHS $\delta^{18}O$ values are taken from Massey et al. (1994a, 1994b), and recalculated using the fractionation equation of Lackey et al. (2005) assuming 74% SiO_2 in the melt. For the mixing lines, mantle-like oxygen and hafnium isotopic values were used (Valley, 2003; Bouvier et al., 2008). The Xigaze ophiolite of southern Tibet was chosen to provide bulk-rock Hf abundances for a mantle-derived end-member of appropriate age (2.1 ppm, Malpas et al., 2003). There is no correlation between samples with the same symbol or colour. Error bars are 2σ for Hf and 2 s.d. for O. (b) Plot adapted from Kemp et al. (2006) highlighting one I-type and two S-type granites from the Lachlan fold belt, and mixing lines between potential metasedimentary and gabbroic end-members.

Zircons in samples 1G02 and 1G03 yielded slightly lower $\delta^{18}O$ values than have previously been reported from bulk-rock GHS data. One zircon from 1G03 also yielded somewhat more negative εHf_{20} than has previously been reported for the GHS.

Two main age groups of 550–450 Ma and 900–800 Ma are observed in the pre-Himalayan zircon core data (Fig. 3), which are similar age ranges to those found in previous detrital zircon studies of the eastern Himalaya (Kemp et al., 2009; Gehrels et al., 2011). A smaller group of Paleoproterozoic cores yielding ages of ~1800 Ma was only found in four samples – 1G02, 1G03, 1247 and CWB16. In addition, several zircons yield ages between these main groups, representing either a mixed age or another, smaller source contribution. The majority of zircons within the 550–450 Ma group have an εHf_t composition of +2.5 to −8, with outliers at +9.5 and −15.5. The majority of zircons in the 900–800 Ma population lie between −7 and −15. The smaller ~1800 Ma group records εHf_t between +8 and −10.

4. Discussion

Of the Oligocene–Miocene aged zircon rims, 97% lie within uncertainty of the GHS metasedimentary Hf–O isotopic field, suggesting that the main source of these melts was the GHS material into which they are now emplaced (Fig. 2). The zircon arrays from individual granites generally vary in $\delta^{18}O$ at relatively constant εHf_{20}. In comparison with the Lachlan fold belt data (Fig. 2 inset), our data do not appear to lie on potential mixing lines drawn between possible GHS compositions and a mantle-derived end-member (Vervoort and Blichert-Toft, 1999; Valley, 2003). One potential explanation is that crust–mantle hybrid magma batches were internally well blended at the scale of individual samples and thus crystallised zircons of limited Hf–O isotope variability. For example sample 1D01 may have formed by mixing between a relatively juvenile magma and a crustal component represented by 1G01. However no samples yield zircons with εHf_{20} values greater than the maximum GHS-field value. We would argue that whilst the GHS field is relatively large, so that zircon compositions lying within it might represent mixtures between sediment of more extreme crustal signature and mantle, evidence from individual granites argues against any such mixing.

Zircons in four samples, 1G02, 1G03, 1251, and CWB16, show significant variations in εHf_{20}, consistent with the interpretation that the melt in these samples has been derived from multiple sources. Of these, data from samples 1251 and CWB16 lie within the GHS field, suggesting they reflect mixing between two different crustal sources within the GHS. For example the most fusible lithologies in the GHS are likely to be pelitic or semi-pelitic in composition, reflecting mudstone and greywacke protoliths respectively, that are likely to have slightly differing isotopic characteristics. One zircon in 1G03 records more negative εHf_{20} values than the bulk GHS, which could suggest mixing between the GHS and an older source. This source could potentially be the Lesser Himalayan Series (LHS) which underthrusts the GHS and is characterised by older (Paleoproterozoic) sedimentary protoliths and significantly older Nd model ages (Ahmad et al., 2000). Furthermore, the presence of Paleoproterozoic zircon cores in samples 1G02, 1G03 and CWB16 could imply that some LHS material has been entrained into these leucogranites, which could explain the variable εHf_{20} signatures seen in these samples. The possibility that the LHS is a significant source to leucogranite generation is precluded by the presence of significant Neoproterozoic core populations, which are not found in the LHS (Gehrels et al., 2011).

Zircons from 1G02 and one zircon each from samples 1D01 and 1G03 also yield lower $\delta^{18}O$ values than the GHS field. These three samples were all collected south of the village of Gasa (Fig. 1), where numerous epidote-bearing calc-silicate lenses are

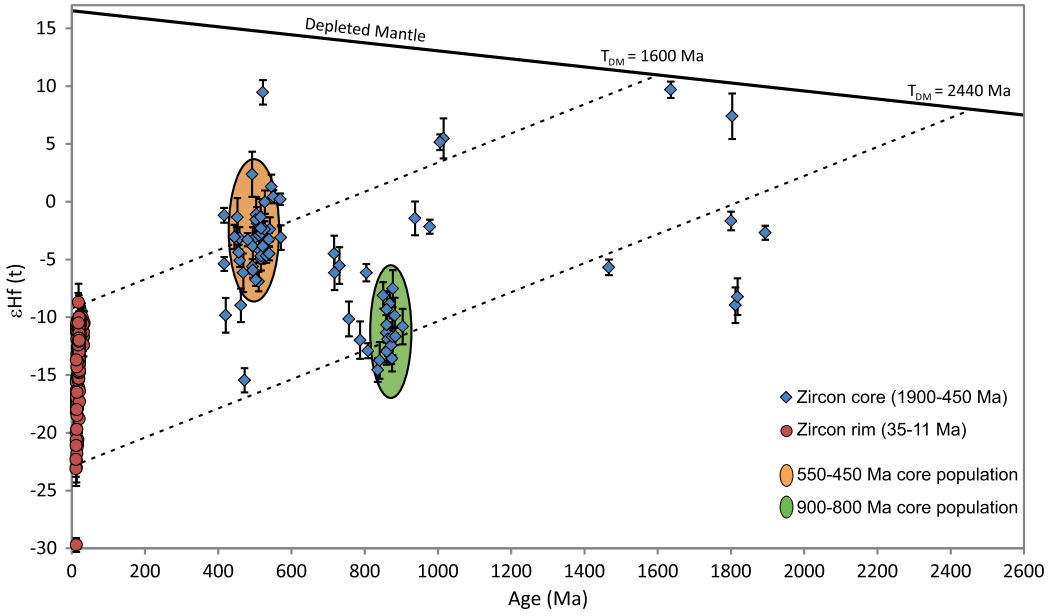

Fig. 3. Plot of εHf_t and U–Pb crystallisation age for core and rim zircon data. Core data plot in two main groups, at 550–450 Ma and 900–800 Ma, with additional zircons plotting at ~1800 Ma and between these groups. Evolution line for the depleted mantle is shown. Evolution lines from core populations are also plotted, assuming a $^{176}Lu/^{177}Hf$ ratio of 0.015. Himalayan-age zircon rim data is bound by these evolution lines, with no positive deviation to a mantle value. Error bars are 2σ uncertainty.

exposed (Gansser, 1983). Epidote-bearing calc-silicates in the Himalaya yield an overall lower bulk-rock $\delta^{18}O$ than the dominant metapelites (Massey et al., 1994a, 1994b), hence a small contribution from calc-silicate material in the source melt could explain the reduced $\delta^{18}O$ in these samples. As calc-silicates are also found throughout the GHS, it is possible that other samples whose zircons express variability in $\delta^{18}O$ with constant εHf_{20} (such as 4D01, 1215 and 1247) have also incorporated calc-silicate material in their source, leading to mixed $\delta^{18}O$ signatures.

Zircon core data may also be employed to assess the relationship between source and melt. Fig. 3 displays the relationship between Himalayan rim and pre-Himalayan core data, with Hf evolution lines based on a $^{176}Lu/^{177}Hf$ ratio of 0.015 (typical of upper continental crust, Griffin et al., 2004). The range of Himalayan-aged zircon εHf_{20} values is entirely constrained by the evolution lines derived from the two most abundant source fields – the 550–450 Ma and 900–800 Ma groups. This suggests that the Himalayan-aged rims derive their Hf isotopic composition solely from these two sources. Furthermore, as there is no positive deviation in the Himalayan-aged rim εHf_{20} data towards a mantle value, it provides additional evidence against the possibility that the mantle contributed to the formation of these zircon rims, and to their host leucogranites.

Heat production in the upper part of the sequence in the central Himalaya, determined from chemical analyses of GHS metasediments, averages at 3.2 μWm^{-3} but can be as high as 7 μWm^{-3}. Values in the lower (unmelted) GHS are lower, ranging from 1–2 μWm^{-3} (Inger and Harris, 1992). This suggests that heat production in the upper parts of the GHS is unusually high allowing internal heating to result in a rapid rise in temperature during crustal thickening. 1D thermal modelling suggests melting of muscovite-bearing metasediments during Himalayan uplift at 15 to 20 Ma (Zhang et al., 2004). 2D thermomechanical modelling of the Himalayan orogen suggests that melting temperatures (>700 °C) could have been attained at the depths of the upper GHS as early as ~30 Ma following crustal thickening that commenced during the Early Eocene (~50 Ma). This heating subsequently lead to widespread granite magma formation at ~20 Ma (Beaumont et al., 2001; Jamieson et al., 2011). More detailed thermal modelling lies outside the scope of this study but the available numerical results demonstrate that a time lag of 30–40 Myr between collision and widespread melt formation within the upper GHS is entirely consistent with the known thermal characteristics of the source rocks identified in this study.

Our results have ramifications for our understanding of crustal growth. Many published crustal growth curves are underpinned by U–Pb, Hf, O data from detrital zircons. These data are used to estimate rates of magmatism and crustal reworking over the geological record (e.g. Dhuime et al., 2012; Hawkesworth et al., 2013). Current crustal growth rates are estimated from juvenile igneous activity in a range of tectonic settings coupled to estimates of mantle-directed crustal recycling (Scholl and von Huene, 2009). Both historic and modern rates are critical to our understanding of plate tectonics and supercontinent cycles throughout the Earth's history. While the majority of magmatic addition (and crustal recycling) occurs at subduction zones, it is thought that a significant proportion of crustal growth occurs during collisional orogenesis at a rate of ~0.2 $km^3\ a^{-1}$ (Scholl and von Huene, 2009; Hawkesworth et al., 2013). However, such conclusions are based largely on data from pre-Tertiary orogenic belts. Our conclusion that widespread felsic magmatism in the Himalayas involved no interaction from the mantle, and therefore no crustal growth, suggests that the estimated current rate of crustal growth may be an overestimate. As the estimated current overall growth rate of the crust is similar to historic rates calculated from detrital zircons (Dhuime et al., 2012), it is possible that growth rates in other tectonic settings are commensurately underestimated, or that recycling rates are also overestimated.

Our data suggest that felsic magmatism linked to substantial crustal thickening within collision zones does not in itself provide evidence for significant crustal growth. Indeed, since regional crustal thickening involving large mature continental lithospheric plates is more likely during Phanerozoic orogenesis, current models for continental crustal growth rate during the Phanerozoic may be over-estimated. A previously-reported slowdown in crustal growth after 0.6 Ga corroborates this suggestion (Belousova et al., 2010). This study stresses the importance of incorporating empirical observations of recent tectonic settings into crustal growth calculations.

5. Conclusions

Overall, the data show that Oligocene–Miocene aged zircons and zircon rims from granites that intrude the high metamorphic grade Greater Himalayan Sequence in Bhutan show limited isotopic variation within individual rock samples, and lie within the field defined by isotopic variability in the GHS. Some zircon populations display isotope trends that are consistent with mixing between two or more metasedimentary sources, but none show trends that are consistent with mixing with a mantle source. Furthermore, εHf_t data from zircon cores suggests the Himalayan-aged rims derived solely from Cambrian and Proterozoic sources, with no positive deviation in rim data towards a mantle value. In addition, no field evidence exists for xenoliths of mafic composition in the Himalayan leucogranites.

The lack of Miocene mantle interaction significantly affects our understanding of the Himalayan orogen. As this removes the possibility of additional heat sources being involved in the melt process, it fails to support the possibility of the 'young' collision model at ~34 Ma (Aitchison et al., 2007). The most likely scenario is that a single collision occurred to form the Himalayan orogeny at ~55–50 Ma (Najman et al., 2010).

Unlike granitic zircon O-Hf studies from other regions, we find no evidence for source contributions from melting of mafic sources or mixing with mantle-derived or more juvenile melts. We therefore conclude that they are pure crustal melts from metasedimentary sources, a conclusion consistent with their bulk geochemical signatures (Le Fort et al., 1987; Harris et al., 1995). The Himalayan leucogranites therefore provide clear evidence that syn-collision S-type granites need not contribute to crustal growth, and further that the presence of such granites within orogenic belts does not require an advective heat source in thermal models for orogenic evolution. The lack of mantle interaction also suggests that current estimates for rates of crustal growth during collisional orogenesis may be overestimated. We also propose that an 'end-member' S-type granite should be defined as a rock whose zircon Hf–O isotopic signatures lie entirely within error of those of its probable source, and where no trajectories to mantle values are observed. These leucogranites are also a more appropriate 'type-locality' for S-type granites than the Lachlan Fold Belt of Australia. Our results have implications for the formation of granites in general, for crustal growth estimates within orogenic belts and for the thermal and mechanical modelling of the Himalayan orogen.

Acknowledgements

T.H. acknowledges funding from NERC CASE studentship NE/K501074/1. C.W. acknowledges funding from a NERC Advanced Fellowship (NE/HO16279/1). Analytical work was funded by NERC facility grants awarded by the EIMF to N.B.W.H. and T.H. (IMF478/0513) and by the NIGFSC to C.W. and T.H. (IP-1403-111). Thanks are extended to D. Regis and D. Young for providing samples and field assistance, A. Wood for assistance with sample preparation at NIGL, and S. Hammond, B. Charlier, D. Regis and C. Mottram for fruitful discussions.

Appendix A. Supplementary material

Supplementary material related to this article can be found online at http://dx.doi.org/10.1016/j.epsl.2017.03.018.

References

Ahmad, T., et al., 2000. Isotopic constraints on the structural relationships between the lesser Himalayan series and the high Himalayan crystalline series, Garhwal Himalaya. Geol. Soc. Am. Bull. 112, 467–477.

Aitchison, J.C., Ali, J.R., Davis, A.M., 2007. When and where did India and Asia collide? J. Geophys. Res., Solid Earth 112, B05423.

Appleby, S.K., et al., 2010. Do S-type granites commonly sample infracrustal sources? New results from an integrated O, U–Pb and Hf isotope study of zircon. Contrib. Mineral. Petrol. 160, 115–132.

Bea, F., Montero, P., González-Lodeiro, F., Talavera, C., 2007. Zircon inheritance reveals exceptionally fast crustal magma generation processes in Central Iberia during the Cambro–Ordovician. J. Petrol. 48, 2327–2339.

Beaumont, C., Jamieson, R.A., Nguyen, M.H., Lee, B., 2001. Himalayan tectonics explained by extrusion of a low-viscosity crustal channel coupled to focused surface denudation. Nature 414 (6865), 738–742.

Belousova, E.A., Kostitsyn, Y.A., Griffin, W.L., Begg, G.C., O'Reilly, S.Y., Pearson, N.J., 2010. The growth of the continental crust: constraints from zircon Hf-isotope data. Lithos 119 (3), 457–466.

Bouvier, A., Vervoort, J.D., Patchett, P.J., 2008. The Lu–Hf and Sm–Nd isotopic composition of CHUR: constraints from unequilibrated chondrites and implications for the bulk composition of terrestrial planets. Earth Planet. Sci. Lett. 273, 48–57.

Chappell, B.W., White, A.J.R., 1974. Two contrasting granite types. Pac. Geol. 8, 173–174.

Collins, W.J., 1996. Lachlan Fold Belt granitoids: products of three-component mixing. Spec. Pap., Geol. Soc. Am. 315, 171–181.

Dhuime, B., Hawkesworth, C.J., Cawood, P.A., Storey, C.D., 2012. A change in the geodynamics of continental growth 3 billion years ago. Science 335 (6074), 1334–1336.

Gansser, A., 1983. Geology of the Bhutan Himalaya. Denkschiften Schweizerischen Naturforschenden Gesellschaft 95, 181.

Gehrels, G., et al., 2011. Detrital zircon geochronology of pre-Tertiary strata in the Tibetan–Himalayan orogen. Tectonics 30 (5).

Gray, C.M., 1984. An isotopic mixing model for the origin of granitic rocks in southeastern Australia. Earth Planet. Sci. Lett. 70 (1), 47–60.

Greenwood, L.V., Argles, T.W., Parrish, R.R., Harris, N.B.W., Warren, C., 2016. The geology and tectonics of central Bhutan. J. Geol. Soc. Lond. 173, 352–369.

Griffin, W.L., Belousova, E.A., Shee, S.R., Pearson, N.J., O'Reilly, S.Y., 2004. Archean crustal evolution in the northern Yilgarn Craton: U–Pb and Hf-isotope evidence from detrital zircons. Precambrian Res. 131 (3), 231–282.

Hanchar, J.M., Watson, E.B., 2003. Zircon saturation thermometry. Rev. Mineral. Geochem. 53, 89–112.

Harris, N., Massey, J., 1994. Decompression and anatexis of Himalayan metapelites. Tectonics 13, 1537–1546.

Harris, N., Ayres, M., Massey, J., 1995. Geochemistry of granitic melts produced during the incongruent melting of muscovite: implications for the extraction of Himalayan leucogranite magmas. J. Geophys. Res., Solid Earth 100, 15767–15777.

Hawkesworth, C., Cawood, P., Dhuime, B., 2013. Continental growth and the crustal record. Tectonophysics 609, 651–660.

Healy, B., Collins, W.J., Richards, S.W., 2004. A hybrid origin for Lachlan S-type granites: the Murrumbidgee Batholith example. Lithos 78, 197–216.

Hu, X., Garzanti, E., Moore, T., Raffi, I., 2015. Direct stratigraphic dating of India–Asia collision onset at the Selandian (middle Paleocene, 59 ± 1 Ma). Geology 43, 859–862.

Inger, S., Harris, N.B.W., 1992. Tectonothermal evolution of the High Himalayan Crystalline Sequence, Langtang Valley, northern Nepal. J. Metamorph. Geol. 10, 439–452.

Inger, S., Harris, N.B.W., 1993. Geochemical constraints on leucogranite magmatism in the Langtang Valley, Nepal Himalaya. J. Petrol. 34 (2), 345–368.

Jackson, S.E., Pearson, N.J., Griffin, W.L., Belousova, E.A., 2004. The application of laser ablation-inductively coupled plasma-mass spectrometry to in situ U–Pb zircon geochronology. Chem. Geol. 211, 47–69.

Jamieson, R.A., Unsworth, M.J., Harris, N.B.W., Rosenberg, C.L., Schulmann, K., 2011. Crustal melting and the flow of mountains. In: Sawyer, E.W., Cesare, B., Brown, M. (Eds.), When the Continental Crust Melts. In: Elements, vol. 7, pp. 251–258.

Kemp, A.I.S., et al., 2006. Exploring the plutonic–volcanic link: a zircon U–Pb, Lu–Hf and O isotope study of paired volcanic and granitic units from southeastern Australia. Trans. R. Soc. Edinb. Earth Sci. 97, 337–355.

Kemp, A.I.S., et al., 2007. Magmatic and crustal differentiation history of granitic rocks from Hf–O isotopes in zircon. Science 315, 980–983.

Kemp, A.I.S., Foster, G.L., Scherstén, A., Whitehouse, M.J., Darling, J., Storey, C., 2009. Concurrent Pb–Hf isotope analysis of zircon by laser ablation multi-collector ICP–MS, with implications for the crustal evolution of Greenland and the Himalayas. Chem. Geol. 261 (3), 244–260.

Lackey, J.S., Valley, J.W., Saleeby, J.B., 2005. Supracrustal input to magmas in the deep crust of Sierra Nevada batholith: evidence from high-$\delta^{18}O$ zircon. Earth Planet. Sci. Lett. 235, 315–330.

Le Fort, P., et al., 1987. Crustal generation of the Himalayan leucogranites. Tectonophysics 134, 39–57.

Loiselle, M.C., Wones, D.R., 1979. Characteristics and origin of anorogenic granites. Abstr. Program – Geol. Soc. Am. 11, 468.

Malpas, J., Zhou, M.F., Robinson, P.T., Reynolds, P.H., 2003. Geochemical and geochronological constraints on the origin and emplacement of the Yarlung Zangbo ophiolites, Southern Tibet. Geol. Soc. (Lond.) Spec. Publ. 218, 191–206.

Massey, J.A., Harmon, R.S., Harris, N.B.W., 1994a. Contrasting retrograde oxygen isotope exchange behaviour and implications: examples from the Langtang Valley, Nepal. J. Metamorph. Geol. 12, 261–272.

Massey, J.A., Reddy, S.M., Harris, N.B.W., Harmon, R.S., 1994b. Correlation between melting, deformation and fluid interaction in the continental crust of the High Himalayas, Langtang Valley, Nepal. Terra Nova 6, 229–237.

McCulloch, M.T., Chappell, B.W., 1982. Nd isotopic characteristics of S- and I-type granites. Earth Planet. Sci. Lett. 58, 51–64.

Medvedev, S., Beaumont, C., 2006. Growth of continental plateaus by channel injection: models designed to address constraints and thermomechanical consistency. Geol. Soc. (Lond.) Spec. Publ. 268, 147–164.

Najman, Y., et al., 2010. Timing of India–Asia collision: geological, biostratigraphic, and palaeomagnetic constraints. J. Geophys. Res., Solid Earth 115, B12416.

Patiño-Douce, A.E., Humphreys, E.D., Johnston, A.D., 1990. Anatexis and metamorphism in tectonically thickened continental crust exemplified by the Sevier hinterland, western North America. Earth Planet. Sci. Lett. 97, 290–315.

Patiño Douce, A.E., Johnston, A.D., 1991. Phase equilibria and melt productivity in the pelitic system: implications for the origin of peraluminous granitoids and aluminous granulites. Contrib. Mineral. Petrol. 107, 202–218.

Roberts, N.M., Spencer, C.J., 2014. The zircon archive of continent formation through time. Geol. Soc. (Lond.) Spec. Publ. 389, 197–225.

Savage, P.S., et al., 2012. The silicon isotope composition of granites. Geochim. Cosmochim. Acta 92, 184–202.

Scholl, D.W., von Huene, R., 2009. Implications of estimated magmatic additions and recycling losses at the subduction zones of accretionary (non-collisional) and collisional (suturing) orogens. Geol. Soc. (Lond.) Spec. Publ. 318 (1), 105–125.

Sláma, J., et al., 2008. Plešovice zircon — a new natural reference material for U–Pb and Hf isotopic microanalysis. Chem. Geol. 249, 1–35.

Spencer, C.J., et al., 2015. Generation and preservation of continental crust in the Grenville Orogeny. Geosci. Front. 6, 357–372.

Teng, F.Z., et al., 2004. Lithium isotopic composition and concentration of the upper continental crust. Geochim. Cosmochim. Acta 68, 4167–4178.

Valley, J.W., 2003. Oxygen isotopes in zircon. Rev. Mineral. Geochem. 53, 343–385.

Vervoort, J.D., Blichert-Toft, J., 1999. Evolution of the depleted mantle: Hf isotope evidence from juvenile rocks through time. Geochim. Cosmochim. Acta 63, 533–556.

Wiedenbeck, M., et al., 1995. Three natural zircon standards for U–Th–Pb, Lu–Hf, trace element and REE analyses. Geostand. Newsl. 19, 1–23.

Wiedenbeck, M., et al., 2004. Further characterisation of the 91500 zircon crystal. Geostand. Geoanal. Res. 28, 9–39.

Woodhead, J.D., Hergt, J.M., 2005. A preliminary appraisal of seven natural zircon reference materials for in situ Hf isotope determination. Geostand. Geoanal. Res. 29, 183–195.

Zhang, H., et al., 2004. Causes and consequences of protracted melting of the mid-crust exposed in the North Himalayan antiform. Earth Planet. Sci. Lett. 228, 195–212.